JOURNAL OF BACTERIOLOGY, Sept. 2003, p. 5086–5095 Vol. 185, No. 17
0021-9193/03/$08.00+0 DOI: 10.1128/JB.185.17.5086–5095.2003

Protein Content of Polyhedral Organelles Involved in Coenzyme B_{12}-Dependent Degradation of 1,2-Propanediol in *Salmonella enterica* Serovar Typhimurium LT2†

Gregory D. Havemann and Thomas A. Bobik*

Department of Microbiology and Cell Science, University of Florida, Gainesville, Florida

Received 11 March 2003/Accepted 21 May 2003

Salmonella enterica **forms polyhedral organelles during coenzyme B_{12}-dependent growth on 1,2-propanediol (1,2-PD). Previously, these organelles were shown to consist of a protein shell partly composed of the PduA protein, the majority of the cell's B_{12}-dependent diol dehydratase, and additional unidentified proteins. In this report, the polyhedral organelles involved in B_{12}-dependent 1,2-PD degradation by *S. enterica* were purified by a combination of detergent extraction and differential and density gradient centrifugation. The course of the purification was monitored by electron microscopy and gel electrophoresis, as well as enzymatic assay of B_{12}-dependent diol dehydratase. Following one- and two-dimensional gel electrophoresis of purified organelles, the identities and relative abundance of their constituent proteins were determined by N-terminal sequencing, protein mass fingerprinting, Western blotting, and densitometry. These analyses indicated that the organelles consisted of at least 15 proteins, including PduABB′CDEGHJKOPTU and one unidentified protein. Seven of the proteins identified (PduABB′JKTU) have some sequence similarity to the shell proteins of carboxysomes (a polyhedral organelle involved in autotrophic CO_2 fixation), suggesting that the *S. enterica* organelles and carboxysomes have a related multiprotein shell. In addition, *S. enterica* organelles contained four enzymes: B_{12}-dependent diol dehydratase, its putative reactivating factor, aldehyde dehydrogenase, and ATP cob(I)alamin adenosyltransferase. This complement of enzymes indicates that the primary catalytic function of the *S. enterica* organelles is the conversion of 1,2-PD to propionyl coenzyme A (which is consistent with our prior proposal that the *S. enterica* organelles function to minimize aldehyde toxicity during growth on 1,2-PD). The possibility that similar protein-bound organelles may be more widespread in nature than currently recognized is discussed.**

The vitamin B_{12} coenzymes adenosyl-B_{12} (Ado-B_{12}) and methyl-B_{12} (CH_3-B_{12}) are required cofactors for at least 15 different enzymes (5, 27, 30). These enzymes have a broad but uneven distribution among living forms and are vital to human health, are essential to the carbon cycle, and have important industrial applications (5, 27, 30). Historically, bacteria have provided excellent model systems for the study of vitamins, and recent investigations with several bacterial systems have found the molecular biology of B_{12}-dependent processes to be unexpectedly complex (9, 27, 29, 34, 35). One of the most surprising findings in this area has been the identification of a polyhedral organelle involved in coenzyme B_{12}-dependent 1,2-propanediol (1,2-PD) degradation by *Salmonella enterica* (9).

Salmonella enterica utilizes 1,2-PD as a carbon and energy source in an Ado-B_{12}-dependent fashion (19). Degradation occurs aerobically, or anaerobically if tetrathionate is added as a terminal electron acceptor (26). Based on biochemical studies, a pathway for 1,2-PD degradation has been proposed (24, 37). Breakdown initiates with the conversion of 1,2-PD to propionaldehyde by Ado-B_{12}-dependent diol dehydratase (1). The propionaldehyde is then reduced to propanol or oxidized to propionic acid via propionyl coenzyme A (propionyl-CoA) and propionyl-phosphate. Reduction of propionaldehyde serves to regenerate NAD from NADH, while its oxidation provides a source of ATP and cell carbon.

Because the pathway of 1,2-PD degradation appeared relatively straightforward, it was somewhat surprising when DNA sequence analyses indicated that the 1,2-PD utilization (*pdu*) locus included 23 genes (9). Of these, six *pdu* genes are thought to encode enzymes needed for the 1,2-PD degradative pathway (*pduCDEPQW*); two are involved in transport and regulation (*pduF* and *pocR*); two are probably used for diol dehydratase reactivation (*pduGH*); one is needed for the conversion of CN-B_{12} to Ado-B_{12} (*pduO*); five are of unknown function (*pduLMSVX*); and seven (*pduABJKNTU*) share similarity to genes needed for the formation of carboxysomes, polyhedral organelles involved in autotrophic CO_2 fixation (8–10, 13, 15, 20, 31, 32).

The finding that the *pdu* locus included several homologues of carboxysome genes led to recent studies which showed that *S. enterica* forms polyhedral organelles during Ado-B_{12}-dependent growth on 1,2-PD (9). Like carboxysomes, the *pdu* organelles are 100 to 150 nm in diameter and are composed of a proteinaceous interior surrounded by a 3- to 4-nm protein shell (9, 17). However, carboxysomes and the *S. enterica* organelles differ in a number of ways. Carboxysomes function to enhance autotrophic growth at low CO_2 concentrations (2, 21, 25, 33), and the carboxysomes of *Halothiobacillus neapolitanus* (which are the best studied) consist of a protein shell composed of at

* Corresponding author. Mailing address: Department of Microbiology and Cell Science, University of Florida, Building 981, Room 1220, Gainesville, FL 32611. Phone: (352) 846-0957. Fax: (352) 392-5922. E-mail: bobik@ufl.edu.

† Florida Agricultural Experiment Station Journal Series no. R-09558.

least six different proteins which encases most of the cell's ribulose 1,5-bisphosphate carboxylase-oxygenase (RuBisCO) (3, 4, 14, 16, 18). In contrast, the organelles of *S. enterica* do not contain RuBisCO but instead consist of Ado-B_{12}-dependent diol dehydratase and a protein shell composed of the PduA protein as well as other unidentified proteins (9, 17). It has been proposed that the *S. enterica* organelles function to minimize aldehyde toxicity by moderating propionaldehyde production through control of Ado-B_{12} availability (17). However, this function has not been established, and a great deal remains to be learned about their structure.

Here we report the purification and structural characterization of the unusual organelles involved in 1,2-PD degradation by *S. enterica*. The analyses performed include one and two-dimensional electrophoresis, immunoblotting, N-terminal sequencing, and protein mass fingerprinting via matrix-assisted laser desorption ionization–time-of-flight mass spectrometry (MALDI-TOF MS). By these methods, 15 proteins of the organelles were identified. These included Ado-B_{12}-dependent diol dehydratase (PduCDE), CoA-dependent propionaldehyde dehydrogenase (PduP), adenosyltransferase (PduO), the large (PduG) and small (PduH) subunits of the putative diol dehydratase-reactivating factor, the PduA shell protein and six additional probable structural proteins (*pduBB′JKTU*), and one unidentified protein. Densitometry results indicated that of the seven possible structural proteins, PduABB′J are the more abundant structural proteins while PduKTU appear to be more minor structural elements. These findings are consistent with a role for the *pdu* organelles in aldehyde detoxification and also show that these organelles represent a complex mode of subcellular organization.

MATERIALS AND METHODS

Chemicals and reagents. 1,2-PD was from Sigma Chemical Company (St. Louis, Mo.), Bacterial Protein Extraction Reagent II (BPER-II) was from Pierce (Rockford, Ill.), and Pefabloc SC was from Pentapharm Ltd. (Basel, Switzerland). Electrophoresis supplies were from Bio-Rad (Hercules, Calif.) unless otherwise stated. Other chemicals were from Fisher Scientific.

Organelle purification. For organelle purification, *S. enterica* serovar Typhimurium LT2 was grown in 2.8-liter Fernbach flasks containing 1 liter of NCE minimal medium (7, 40) supplemented with 1% succinate and 0.4% 1,2-PD, but without added B_{12}. The inoculum was a 5-ml Luria-Bertani broth culture, and incubation was at 37°C with shaking at 275 rpm. Under these conditions, growth is supported by succinate but the 1,2-PD is not metabolized, assuring continued high induction of the *pdu* operon (10, 15). After cultures reached late log phase (optical density at 600 nm between 1 and 1.2), cells from 2 liters of medium were harvested by centrifugation at 4,000 × *g* for 10 min at room temperature. The pelleted cells (5 to 6 g) were washed with 300 ml of lysozyme buffer (50 mM Tris-HCl, 0.6 M sucrose, 5 mM EDTA, 0.2% 1,2-PD [pH 8.0]), resuspended in 30 ml of the same buffer containing lysozyme (2 mg/ml), and incubated at 37°C for 2 h with occasional agitation. Subsequent to digestion with lysozyme all steps were performed at 0 to 4°C. Cells were pelleted by centrifugation (7,740 × *g*, 15 min), washed with lysozyme buffer and resuspended in sonication buffer (50 mM Tris-HCl, 2 mM EDTA, 0.2% 1,2-PD [pH 8.0]) at a concentration of 0.1 g of wet cell mass per ml. Cells were then lysed by sonication (four 30-s bursts with 1-min cooling intervals on ice) using a VirSonic 300 sonicator (The Virtis Company, Inc., Gardiner, N.Y.) with a 10-mm-diameter disruptor horn and an output setting of 10. After sonication, the crude cell extract was diluted with an equal amount of BPER-II supplemented with 400 mM NaCl and 20 mM $MgCl_2$ and then incubated at 4°C for 30 min on a rotary shaker set at 18 rpm. Unlysed cells and cell debris were removed by centrifugation at 12,000 × *g* for 10 min, and the resulting supernatant was then subjected to high-speed centrifugation (Beckman SW-27 rotor, 49,000 × *g*, 90 min). The pellet was resuspended in 5 ml of TEMP buffer (50 mM Tris-HCl, 1 mM EDTA, 10 mM $MgCl_2$, 0.2% 1,2-PD [pH 8.0]) and then clarified by low-speed centrifugation (12,000 × *g*, 10 min). The clarified preparation was layered over two 35-ml, 35-to-65%, continuous sucrose gradients in 38.5-ml tubes and centrifuged for 12 h (Beckman SW-27 rotor, 104,000 × *g*). The polyhedral organelles formed a white translucent band about two-thirds of the way down the centrifuge tube, whereas membrane fragments and amorphous debris formed an opaque tan band below. The fraction containing the polyhedra was collected from each gradient with a plastic pipette, diluted to 38.5 ml with TEMP buffer, and centrifuged at 52,000 × *g* for 90 min. The pellets were resuspended in 1 ml of TEMP buffer and clarified by centrifugation for 10 min at 12,000 × *g* using an Eppendorf 5415C microcentrifuge. The supernatant containing the purified organelles was carefully removed and stored at 4°C prior to analysis.

General protein and molecular methods. Protein concentration was determined using the Bio-Rad protein assay and bovine serum albumin as the standard. Other molecular and protein methods were performed as previously described (28).

Electron microscopy. Samples of polyhedral organelles were placed on 300 or 400 mesh copper grids, fixed by adding an equal amount of Trump's reagent (22) and incubating at room temperature for 5 min., washed with double-deionized H_2O, and then stained with 1% uranyl acetate. Samples were viewed and photographed with a Zeiss EM-10CA transmission electron microscope.

Western blots. Purified polyhedral organelles (20 μg) were concentrated using a Vivaspin centrifugal filtration device (Sartorius AG, Goettingen, Germany) with a 5,000-molecular-weight cutoff and then subjected to sodium dodecyl sulfate polyacrylamide gel electrophoresis (SDS-PAGE) using a 4-to-20% gradient gel (Bio-Rad). After electrophoresis, the proteins were transferred to a Hybond P membrane (Amersham Biosciences Corp., Piscataway, N.J.) and probed as described previously (17) using primary antisera at the following dilutions: anti-PduAJ, 1:3,500; anti-diol dehydratase, 1:1,000; anti-PduA, 1:3,500; anti-PduO, 1:1,000; and anti-PduP, 1:1,000.

Diol dehydratase assays. Diol dehydratase assays were performed using the 3-methyl-2-benzothiazolinone hydrazone method as previously described (39). One unit of activity is defined as the amount of enzyme that catalyzes the formation of 1 μmol of propionaldehyde per min per mg protein.

Glycoprotein staining. To test for the presence of glycosylated proteins, Pierce glycosylation stain was used according to the manufacturer's instructions.

N-terminal sequencing. Prior to N-terminal sequencing, organelle proteins were separated by two-dimensional (2D) electrophoresis that employed isoelectric focusing and SDS-PAGE (2D-IEF-SDS-PAGE). Purified polyhedral organelles (230 μg) were concentrated to a 20-μl volume using a Vivaspin filtration device (Sartorius AG) with a 5,000-molecular-weight cutoff and mixed with 150 μl of rehydration solution: 7 M urea, 2 M thiourea, 4% 3-[(3-sholamidopropyl)-dimethylammonio]-1-propanesulfonate (CHAPS), 0.1% SDS, 65 mM dithiothreitol, and 1% immobilized pH gradient (IPG) buffer, pH 3 to 10 (Amersham Biosciences Corp). This sample was then used to rehydrate a 7-cm nonlinear pH 3 to 10 IPG strip (Amersham Biosciences Corp.) and isoelectric focusing was performed at 19° C, and 3,500 V, for 63 V · h. Subsequent to isoelectric focusing, the IPG strip was equilibrated with 50 mM Tris-HCl (pH 6.8), 6 M urea, 30% (vol/vol) glycerol, 2% (wt/vol) SDS, 2.5% iodoacetamide, and a trace amount of bromophenol blue. The strip was then sealed on top of a 4-to-20% Tris-glycine gel (10 by 10 cm; Invitrogen, Carlsbad, Calif.) with warm 0.5% agarose made in 25 mM Tris (pH 8.3), 192 mM glycine, and 0.1% SDS. The gel was run for 20 min at 20 V to load the sample and then an additional 90 min at 125 V to resolve the organelle proteins. After electrophoresis, the organelle proteins were transferred to an Immobilon P membrane (Millipore, Billerica, Mass.) by trans-blotting (14.5 h at 20 V and 4°C) and stained with Coomassie brilliant blue R-250. N-terminal sequencing of the organelle proteins separated by 2D PAGE was performed by the University of Florida, Interdisciplinary Center for Biotechnology Research, Protein Chemistry Core Facility using an Applied Biosystems model 494 HT sequencer and standard blot cartridge cycles.

MALDI-TOF MS. The protein components of purified polyhedral organelles (115 μg) were separated by 2D-IEF-SDS-PAGE as described above, but with the following modifications. The IEF dimension employed a 17-cm linear pH 4 to 7 IPG strip (Bio-Rad) and was focused for a total of 95 kV · h. After the IEF dimension, the IPG strip was sealed onto an 8-to-16% polyacrylamide gel (18.3 by 19.3 cm; Bio-Rad) and run for 20 min at 10 mA to load the sample and then another 5 to 6 h at 24 mA to resolve the organelle proteins. Following 2D electrophoresis, the gel was stained with colloidal blue (Genomic Solutions, Ann Arbor, Mich.) and organelle proteins were excised, washed, dried, digested with trypsin, purified using a Millipore ZipTip, and then analyzed by MALDI-TOF MS.

For MS, a calibration mixture of Angiotensin I, ACTH (clip 1 to 17), and ACTH (clip 18 to 39) (Applied Biosystems, Foster City, Calif.) was prepared according to the manufacturer instructions. It was combined with the sample as

an internal standard at a concentration of 1 pmol/μl each protein standard. Tryptic digests were cocrystallized with a matrix of α-cyano-4-hydroxycinnamic acid (Aldrich, St. Louis, Mo.) and analyzed using an Applied Biosystems Voyager-DE Pro MALDI-TOF mass spectrometer operated in the delayed-extraction, reflector mode. This instrument was equipped with a nitrogen laser delivering pulses of UV light (337 nm) and spectra from 100 individual laser shots were collected for each sample. An accelerating voltage of 20 kV, grid voltage of 72%, and extraction delay time of 200 ns were used.

Peptide mass fingerprinting. Two Web-based programs dedicated to protein mass-fingerprinting were used to analyze MALDI-TOF spectra: MS-Fit (http://prospector.ucsf.edu), and Profound (http://129.85.19.192/profound_bin/webProFound.exe) (42). Profound was used to search the NCBI nonredundant protein database, and MS-Fit was used to search one or more of the following databases: Swiss-Prot, GenBank (Genpept), and the NCBI nonredundant database. The following standard parameters were used with both programs: charge state, MH^+; protein mass range, 1 to 100 kDa; all species allowed; full range of pI; one missed cleavage allowed; possible modification of cysteine by acrylamide or carbamidomethylation; possible modification of methionine by oxidation; and peptide mass tolerance of ±50 ppm. Possible adjustments to the above parameters included the following: the protein mass range and pI range were narrowed or extended according to the 2D gel information; *S. enterica* serovar Typhimurium species was selected, if allowable; and the number of missed cleavages allowed was increased if larger peptides were present in the spectra. The number of tryptic peptides included in the search was determined as follows: the peptide masses from the spectra were corrected for isotopic content and ordered according to peak intensity, the threshold for peak detection was set at 2% Base Peak Intensity to filter out noise and then the entire list was uploaded to the MS-Fit or Profound search program. Calibration standards, trypsin autoproteolysis peptides, and possibly known keratin peaks were placed on an exclusion list and not included in the database search. Possible adjustments to the peptide list included the use of fewer peptides if review of raw spectra showed very few peptides above the baseline noise and/or a second search listing only the most intense peaks (top 5, 10, 20, etc.).

Densitometry analysis. Organelle proteins were resolved by 2D-IEF-SDS-PAGE as described above under "N-terminal sequencing" with the following changes. The organelle preparation used contained 17 μg of protein, and the IEF buffer contained a lower concentration of CHAPS (2%) and was supplemented with 1% dodecyl-maltoside. Following 2D electrophoresis, staining was done with Bio-Rad Sypro Ruby protein gel stain, and the relative amounts of organelle proteins were quantitated using an IS-1000 Digital Imaging system (Alpha Innotech Corporation, San Leandro, Calif.).

RESULTS

Purification of polyhedral organelles. The polyhedral organelles involved in 1,2-PD degradation were purified by detergent treatment, and differential and density gradient centrifugation. The progress of the purification was followed by electron microscopy (Fig. 1) SDS-PAGE (Fig. 2) and assay of B_{12}-dependent diol dehydratase (Table 1) an enzyme previously shown to be associated with these organelles (9, 17).

Electron microscopy. Electron microscopy showed that lysis by sonication effectively released the polyhedral organelles. Prolonged treatment of cells with lysozyme and EDTA prior to sonication produced extracts in which polyhedra were better separated from membrane fragments and amorphous debris. Sonication gave a higher yield of purified polyhedra than did lysis of cells using the French press. In lysates generated by sonication, polyhedra appeared to be bound to the outside of membrane vesicles whereas in lysates generated using a French Press, they were mainly encased within membrane vesicles (which apparently interfered with purification). It was important to exclude $MgCl_2$ from the lysis buffer, because otherwise the polyhedral organelles pelleted with the unbroken cells and cell debris in the initial centrifugation step.

After sonication, soluble extracts were treated with the proprietary detergent BPER-II, sodium chloride, and magnesium chloride and centrifuged at 12,000 × *g*. This removed the majority of lipid vesicles and separated the polyhedra from the remaining vesicles and glycogen rosettes. The subsequent 48,000 × *g* centrifugation yielded a pellet highly enriched in polyhedra and separated from soluble proteins, while the final low-speed and sucrose density gradient centrifugation steps removed the remaining high-molecular-weight contaminants.

Electron microscopy indicated that the purified organelles were nearly homogenous (Fig. 1). Purified preparations contained many polyhedra, but no cells, membrane vesicles, or glycogen rosettes were observed. The polyhedral organelles ranged in size from 100 to 150 nm in diameter and had a 3- to 4-nm-thick shell surrounding a heterogeneous interior. The general appearance of the polyhedra remained unchanged

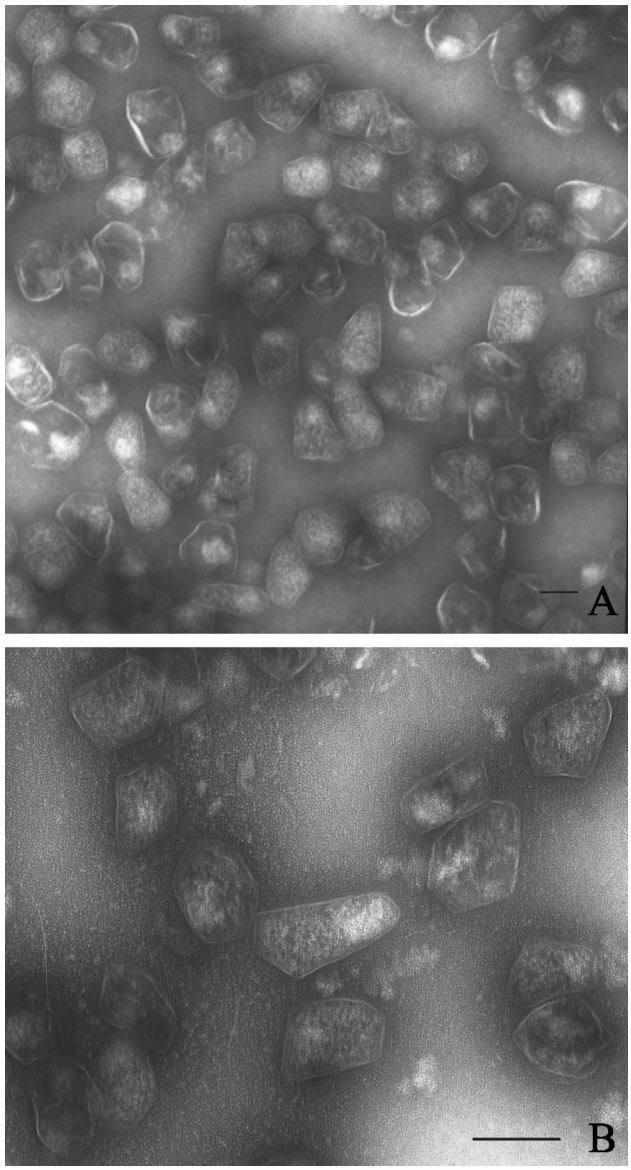

FIG. 1. Electron micrographs of polyhedral organelles purified from *S. enterica*. (A) Magnification, ×53,000. (B) Magnification, ×122,000. The marker bars are 100 nm. Prior to electron microscopy, organelles were fixed with Trump's reagent and then negatively stained with uranyl-acetate.

TABLE 1. Diol dehydratase activity during organelle purification

Sample	Protein (mg)	Activity (μmol/min)[a]	Sp act (μmol/min/mg)[a]	Yield (%)	Purification (fold)
Crude extract	500	1,346	2.7	100	1
Detergent/salts treatment	370.6	1,000	2.7	74.3	1
Supernatant (12,000 × *g*)	357	573	1.6	42.6	0.6
Pellet (48,000 × *g*)	9.4	194	20.8	14.4	7.7
Supernatant (12,000 × *g*)	7	195	27.9	14.5	10.3
Sucrose density gradient	0.6	16	27.5	1.2	10.2

[a] Activities and specific activities were determined by measuring the amount of propionaldehyde formed using the assay as described in Materials and Methods.

throughout the purification. Furthermore, the majority of the polyhedra appeared to be intact and only a small number of broken organelles were observed. In this regard, we point out that fixation prior to negative staining (as described in Materials and Methods) was required to prevent breakdown of the polyhedral organelles during electron microscopy.

SDS-PAGE analysis. The progress of the polyhedral organelle purification was also followed by SDS-PAGE (Fig. 2). Purified organelles were found to be composed of at least 14 proteins with molecular masses ranging from 10.6 to 58.6 kDa (Fig. 2, lane 7). Among these proteins the 10.6-, 11.1-, 17.6-, 27.2-, 29.5-, 38.5-, 42.6-, 51.9-, and 58.6-kDa proteins appeared to be the most abundant. These major protein components of the polyhedra were not easily observed in the crude lysate (Fig. 2, lane 2), the BPER-II-extracted lysate (Fig. 2, lane 3), or the 12,000 × *g* supernatant (Fig. 2, lane 4). However, they became apparent in the 48,000 × *g* pellet (Fig. 2, lane 5) and were further purified following low-speed (Fig. 2, lane 6) and sucrose gradient centrifugation (Fig. 2, lane 7).

Diol dehydratase activity of the polyhedral organelles. Since diol dehydratase was previously shown to be associated with the polyhedral organelles (9, 17), the activity of this enzyme was also used to monitor the organelle purification (Table 1). The specific activity of diol dehydratase was unchanged by the detergent treatment, but this step was necessary to remove lipid vesicles. The 12,000 × *g* centrifugation that followed the detergent treatment resulted in a small decrease in the specific activity of diol dehydratase. However, this step was needed to remove aggregates, which included many organelles that were not released from vesicles by the detergent treatment. Following aggregate removal, the polyhedral organelles were pelleted by centrifugation at 48,000 × *g*, resuspended in buffer, and clarified by a second centrifugation at 12,000 × *g*. These two steps proved very effective and increased the specific activity of diol dehydratase from 1.6 to 27.9 μmol/min/mg. The final sucrose density gradient step typically resulted in a slight drop in the specific activity of diol dehydratase (Table 1). The reason is uncertain. It may have been due to removal of an unknown factor that enhances diol dehydratase activity or due to partial enzyme inactivation.

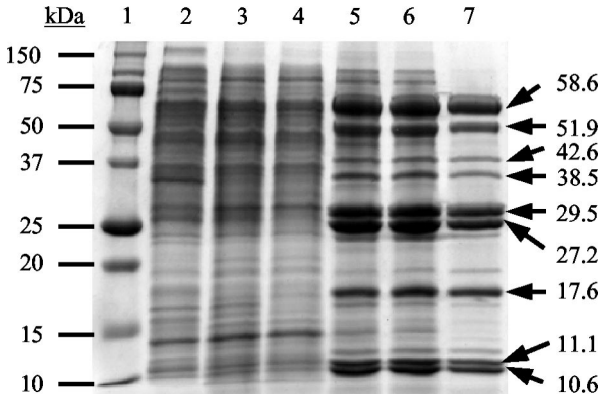

FIG. 2. Analysis of the organelle purification protocol by SDS-PAGE. Lane 1, molecular mass markers; lane 2, crude lysate; lane 3, detergent-treated crude lysate; lane 4, supernatant from centrifugation at 12,000 × *g*; lane 5, pellet from centrifugation at 48,000 × *g*; lane 6, clarified supernatant from centrifugation at 12,000 × *g*; lane 7, density gradient-purified polyhedral organelles. Molecular masses in kilodaltons are shown at the left. Lanes 2 to 7 each contained 20 μg of protein.

For the complete purification, the specific activity of diol dehydratase increased approximately 10-fold, from 2.7 to 27.5 μmol/min/mg protein (Table 1). This indicates that the polyhedral organelles constitute about 10% of the total cell protein, which is consistent with previous electron microscopy, which showed that these structures occupy a significant portion of the cytoplasm of *S. enterica* grown under the conditions used for organelle purification (9, 17).

Western blot analysis of purified polyhedral organelles. To examine their composition, Western blots were performed on purified polyhedral organelles using antisera against diol dehydratase (PduCDE) and the PduAJOP proteins. An antiserum previously shown to be specific for the PduA protein (17) recognized a single band at 11 kDa (Fig. 3 lane 3). This is near the expected value for PduA (9.6-kDa), indicating that this protein is a component of the purified organelles. A second antiserum, shown in a prior study to react with both the PduA and PduJ proteins (17), recognized one band at 11 kDa (PduA) as well as a second band near the predicted molecular mass of PduJ (10.6 kDa) (Fig. 3, lane 4). Thus, it appears that the PduJ protein is also an organelle component.

In further serological tests, PduO and PduP antisera were found to recognize proteins of 39 and 52 kDa, as well as some additional proteins (Fig. 3, lanes 6 and 7). The proteins at 39 and 52 kDa had molecular masses near the predicted values for PduO and PduP (36.8, and 49 kDa) and were unreactive with preimmune sera in control experiments indicating that they likely represent the PduO and PduP proteins, respectively. The additional protein bands recognized by the PduO and PduP antisera appeared to be nonspecific, since preimmune sera reacted with protein bands of similar molecular masses (data

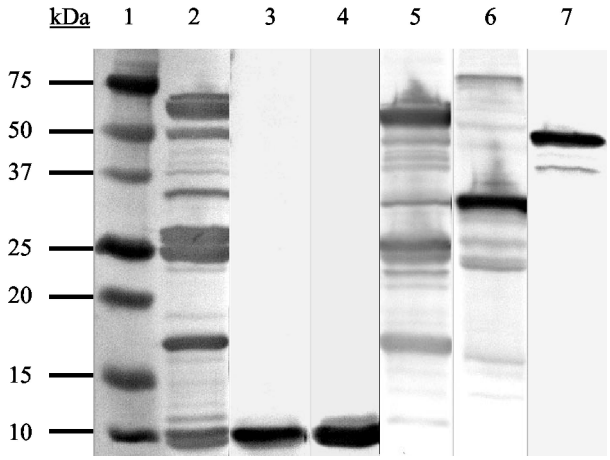

FIG. 3. Western analysis of purified polyhedral organelles. Lane 1, molecular mass markers; lanes 2 to 7 each contained 20 μg of purified polyhedral organelles. Lane 2 was stained with Coomassie brilliant blue and lanes 3 to 7 were probed with the following antisera: lane 3, anti-PduA; lane 4, anti-PduAJ; lane 5, anti-diol dehydratase; lane 6, anti-PduO; lane 7, anti-PduP.

not shown). Hence, these results indicated that the PduO and PduP proteins are part of the purified organelles.

The reaction of purified organelles with anti-diol dehydratase antibody was also tested. This antibody preparation reacted with proteins of 58.6, 30, and 18 kDa (Fig. 3, lane 5). These are the approximate sizes of the three subunits of diol dehydratase (60.3, 24.2, and 19.1 kDa). Prior studies showed that the antiserum used reacts with diol dehydratase (9, 17, 36), but clearly there was also some cross-reactivity, as a number of other protein bands were recognized. Nonetheless, three protein bands near the expected molecular masses for the three subunits of diol dehydratase were identified supporting the enzyme assays described above which indicated that diol dehydratase is associated with the purified organelles.

Glycoprotein staining of organelle proteins. Prior studies showed that the Csos2 protein of carboxysomes is glycosylated (3, 18). Since some components of the *pdu* organelles share homology with the carboxysome proteins, we tested the polyhedral organelles purified from *S. enterica* for the presence of glycoproteins. Organelles proteins were separated by SDS-PAGE and stained for glycoproteins using a commercial kit that is based on the periodic acid-Schiff staining method (41). No glycosylated proteins were detected in the polyhedral organelle preparation (20 μg); however, glycosylation was detected in the positive control, 20 μg horseradish peroxidase (data not shown).

Two-dimensional electrophoresis of purified polyhedral organelles. Samples of purified polyhedral organelles were separated by 2D-IEF-SDS-PAGE (Fig. 4) Seventeen major spots (spots 1 to 12, 16, 18, and 20 to 22) and five minor protein spots (spots 13 to 15 and 17 and 19) were observed. Each protein present in Fig. 4 was reproducibly observed following 2D electrophoresis of three different organelle preparations.

N-terminal sequencing. Subsequent to 2D electrophoresis, the identities of the most intense protein spots were determined by Edman sequential N-terminal degradation followed by sequence similarity searching against the *S. enterica* genome (Table 2) N-terminal sequencing was carried out on the protein spots 1, 3, 10, 12, 16, 21 and 22. Spots 3, 16, 21, and 22 were identified as the PduC, PduE, PduA, and PduJ proteins, respectively, confirming the results of the Western blotting experiments described above. The N-terminal sequence of protein spots 1 and 10 identified these proteins as PduG and PduB, respectively. Surprisingly, spot 12 corresponded to a shorter version of the PduB protein (PduB′) that lacked 37 N-terminal amino acids. Examination of the DNA sequence of the *pduB* gene revealed potential start sites for each protein with an appropriate ATG and Shine-Dalgarno sequence; thus, it appears that *pduB* and *pduB′* represent overlapping genes although at this time posttranslational proteolytic processing remains a possibility. In addition, both of these proteins appear to have the methionine cleaved after translation.

Protein mass fingerprinting. Protein mass fingerprinting was also employed to determine the identities of the organelle proteins resolved by 2D electrophoresis. Proteins corresponding to spots 1 to 9, 11, 13 to 15, and 17 to 20, (Fig. 4) were identified (Table 3) and each spot corresponded to a protein encoded by the *pdu* operon (PduBB′CDEGHJKOPTU). For spot 4, the sequence coverage using both MS-Fit and Profound was $< 25\%$. Nonetheless, it is likely that this spot was composed of the PduP protein, since its mass spectrum was very similar to those of spots 5 and 6, which showed a significant match to the theoretical spectrum for PduP (data not shown).

In addition to PduP, there were several other instances in which more than one protein spot observed by 2D electrophoresis corresponded to the same *pdu* protein (Table 3). This indicated that some organelle proteins existed in different forms during electrophoresis, and could have resulted from incomplete denaturation of the polyhedral organelles prior to isoelectric focusing, from the tight association of lipids or proteins, or from covalent modification. To break down possible noncovalent interactions, dodecyl-maltoside was included in the isoelectric focusing step and the 2-D electrophoresis was repeated. Under these conditions single spots were observed for PduC, PduB, and PduB′, but PduK, PduJ, and PduP were still represented by multiple spots (data not shown). Hence, in the cases of PduK, PduJ, and PduP, posttranslational modification is a possibility.

Unidentified proteins of the purified polyhedral organelles. Each protein spot in Fig. 4 was assigned an identity, with the exception of 19. This spot had an apparent pI of 6.8 and an observed molecular mass of 8.6-kDa. These values do not match well to any known *pdu* protein and protein mass fingerprinting did not match this spot to any protein found in the *S. enterica* genome.

Relative abundance, molecular mass, and pI values of polyhedral organelle proteins separated by 2D electrophoresis. Following 2D electrophoresis of the purified organelles, the molecular mass, and pI values for each organelle protein were determined. In addition, protein spots were quantitated by densitometry so that the relative abundance of each organelle protein could be determined (Table 4) Of the presumed organelle structural proteins, PduABB′J were major components and PduKTU were minor components, both in terms of percent of total protein and molar ratios, the latter of which were as follows: J:A:B′:B:K:T:U = 15:10:7:6:1:1:2.

Of the organelle enzymes, diol dehydratase (PduCDE) was

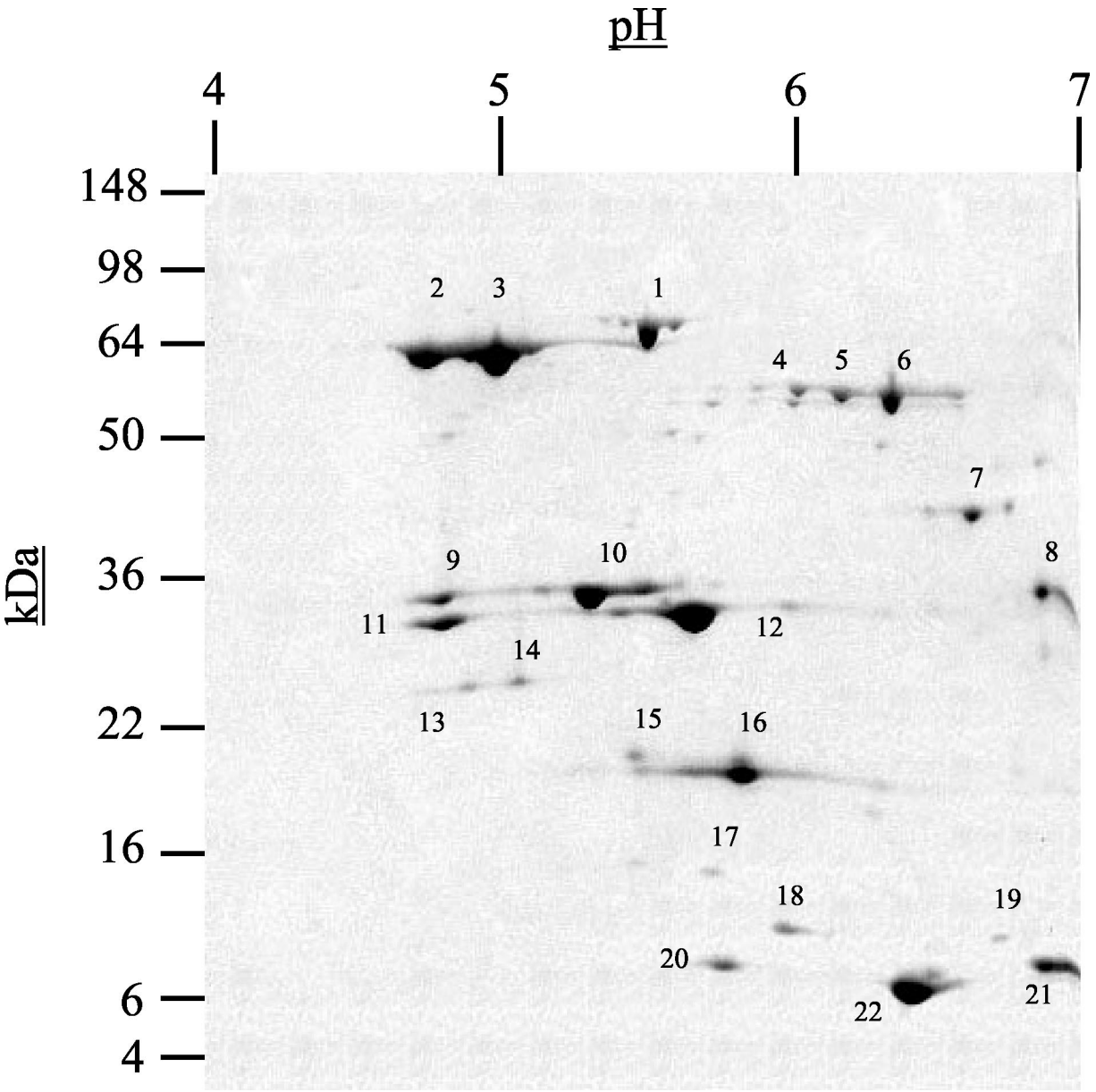

FIG. 4. Two-dimensional electrophoresis of purified polyhedral organelles of *S. enterica*. A purified polyhedral organelle preparation (115 μg of protein) was subjected to 2D-IEF-SDS-PAGE followed by colloidal blue staining. Molecular mass is indicated to the left and IEF pH at the top of the gel.

most abundant. The approximate ratio of the C subunit of diol dehydratase to PduP, PduG, PduH, and PduO was 8:4:2:2:1. This stoichiometry seems reasonable for a set of enzymes that may function as a specific complex although this ratio may not be exact due to the possibility of dye-binding variability. The approximate molar ratios for the subunits of diol dehydratase (PduCDE) and the putative diol dehydratase reactivating factor (PduGH) were 2:1:2 and 2:1, respectively. These ratios are different than the reported subunit compositions of homologous enzymes from *Klebsiella* spp. which are 2:2:2 for diol dehydratase and 2:2 for the reactivating factor (23, 38). It seems most likely that this disparity is due to dye-binding variability; however, the possibility that the composition of diol

TABLE 2. Proteins identified using N-terminal sequencing

Protein analyzed[a]	Determined N-terminal sequence	Matching N-terminal sequence	Identity assigned
1	MRYIAGL	MRYIAGL	PduG
3	MRSKRFE	MRSKRFE	PduC
10	SSNELVE	MSSNELV	PduB
12	AEKSCSL	MAEKSCS	PduB′
16	MNTDAIE	MNTDAIE	PduE
21	MQQEALG	MQQEALG	PduA
22	MNNALGL	MNNALGL	PduJ

[a] The numbers in column 1 refer to the protein spots similarly numbered in Fig. 4.

TABLE 3. Results of peptide mass fingerprinting[a]

Protein analyzed	Identity assigned	NCBI accession no.	MS-Fit analysis			Profound analysis	
			No. of peptides matched	MOWSE score	% Sequence coverage	*Z* score	% Sequence coverage
1	PduG	16765373	15	5.657E+07	29	2.33	40
2	PduC	2587029	17	4.674E+07	31	2.43	31
3	PduC	16765370	6	1.951E+03	16	2.43	52
4	PduP	16765381	6	89.1	15	1.82	16
5	PduP	16765381	15	1.622E+05	39	2.33	47
6	PduP	16765381	15	1.3E+07	36	2.27	54
7	PduO	16765380	10	3.331E+06	43	2.35	52
8	PduD	16765371	7	1.371E+04	28	2.43	22
9	PduB	2587033	26	3.567E+04	47	2.43	44
10	ND						
11	PduB′	16765369	8	3.43E+03	43	2.03	44
12	ND						
13	PduK	16765376	6	2.42E+03	53	1.74	39
14	PduK	16765376	6	2.42E+03	53	2.12	39
15	PduT	16765384	9	2.209E+05	42	2.43	39
16	ND						
17	NS						
18	PduU	16760987-	16	1.262E+08	63	1.74	63
19	PduH	16765374				2.43	28
20	PduJ	16760978	8	2.24E+05	78	2.33	78
21	ND						
22	ND						

[a] The numbers in column 1 refer to the protein spots similarly numbered in Fig. 4. Both the MS-Fit and Profound programs were used to compare the MALDI-TOF MS data obtained for organelle proteins to predicted spectra for proteins present in the GenBank and Swiss-Prot databases. A match was considered significant if the MOWSE score was at least 1e+003 (MS-Fit) or the *Z* score was at least 1.65 (Profound), and the sequence coverage was at least 25%. Abbreviations: ND, not determined; NS, no significant matches.

dehydratase and its reactivating factor differ when these enzymes are associated with polyhedral organelles, or between *Salmonella* and *Klebsiella*, cannot be ruled out.

DISCUSSION

Previously, we established that *S. enterica* forms polyhedral organelles during Ado-B_{12}-dependent growth on 1,2-PD (9, 17). Immunolabeling studies demonstrated that these organelles consisted of a protein shell (partly composed of the PduA protein), the majority of the cell's B_{12}-dependent diol dehydratase, and additional unidentified proteins (9, 17). In this report, we purified the polyhedral organelles involved in 1,2-PD degradation by *S. enterica* and showed that they consist of at least 15 proteins (PduABB′CDEGHJKOPTU and one unidentified protein).

TABLE 4. Molecular mass, pI, and densitometry analyses

Protein	Molecular mass (kDa)		pI		% Total protein	Molar ratio
	Observed	Calculated[a]	Observed[b]	Calculated[a]		
PduG	68.8	64.5	5.5	5.5	5.4	2
PduC	65.3	60.3	4.8–5	5	20.8	8.5
PduP	52.9	49.0	6.0–6.4	6.3	8	4
PduO	36.3	36.8	6.6	7.3	3.6	2.5
PduB	25.6	28.0	4.8–5.3	5.2	12.8	11.5
PduD	25.6	24.2	6.9[c]	8.9	4.8	5
PduB′	23.0	24.0	4.8–5.7	5.6	12.1	12.5
PduK	16.4	16.8	4.9–5.3	5.2	1.6	2.5
PduT	16.4	19.1	5.5	5.9	1.6	2
PduE	16.4	19.1	5.8	5.7	7.9	10.3
Spot17	9.0	ND[d]	5.7	ND	0.8	ND
PduU	8.6	12.5	6	6.1	1.5	3
PduH	8.6	13.4	6.8	7	0.6	1
PduA	7.7	9.6	6.9[c]	7.4	7.5	19.5
PduJ	7.5–7.7	9.0	5.8–6.4	6.5	11	30.5

[a] Calculated from the DNA sequence.
[b] The isoelectric point of each protein was determined from the gel pictured in Fig. 4. Both the molecular masses and the relative protein amounts were calculated from a similar gel supplemented with dodecyl-maltoside to reduce streaking and stained with Sypro Ruby, which has an extended linear range (6). In cases where multiple protein spots corresponded to a single protein, a range is given for the observed pI.
[c] The pI values of PduA and PduD could not be accurately determined experimentally because both proteins focused at the upper limit of the pH range for the gel employed for pI determination (pH 7) and both have calculated pI values above 7.
[d] ND, not determined.

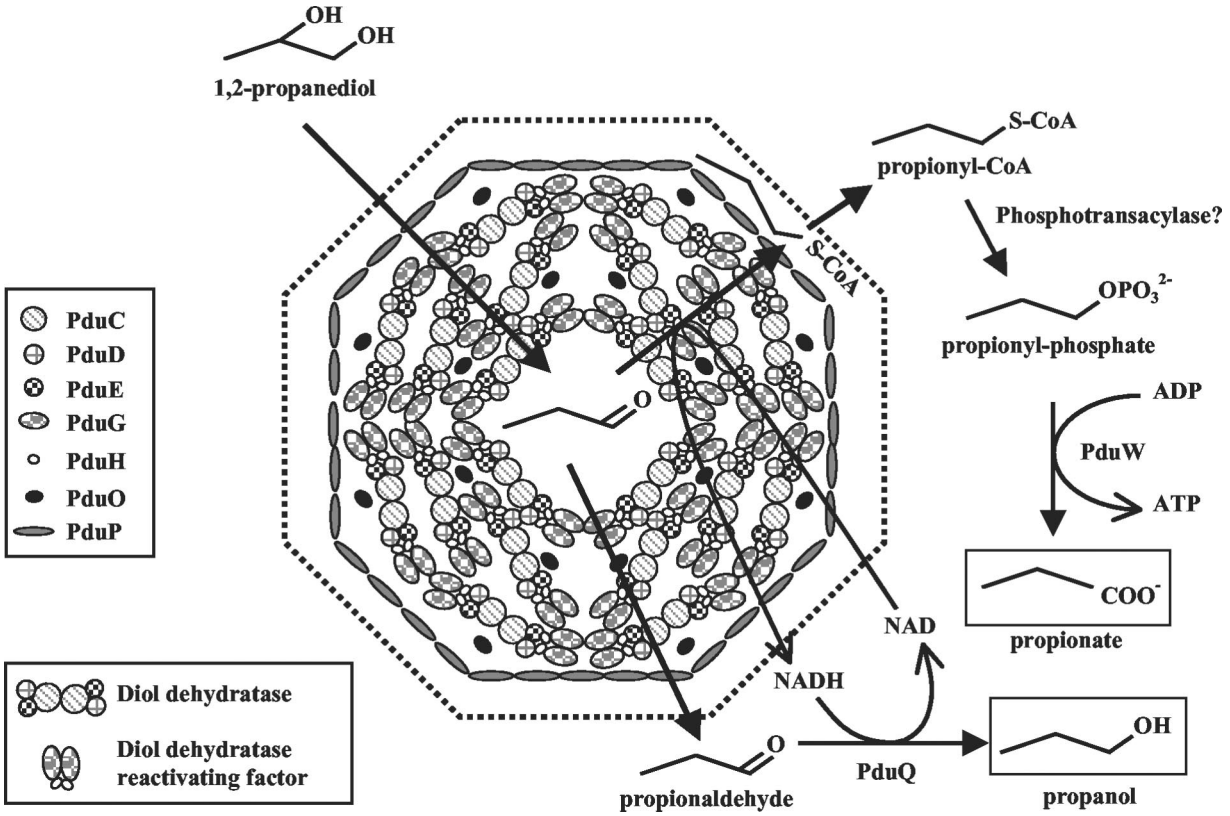

FIG. 5. A model for the role of the *pdu* organelles in 1,2-PD degradation. The dashed line indicates the multiprotein shell of the organelle. The enzymes of the organelle are indicated graphically and in the legend. The pathway of 1,2-PD degradation is also shown. The proposed function of the organelles is to protect cytoplasmic components from the cytotoxic effects of propionaldehyde.

The best studied polyhedral organelles, the carboxysomes of *H. neapolitanus*, are composed of at least 9 proteins: six shell proteins, Csos1A, Csos1B, Csos1C, Csos2A, Csos2B, and Csos3; one protein of unknown function; and the large and small subunits of RuBisCO, CbbL, and CbbS (14, 18). Thus far, the only protein shown to be part of the shell of the *S. enterica* organelles is the PduA protein (17), which is a homologue of the Csos1A, Csos1B, and Csos1C proteins (9, 31). However, the PduJKT proteins also have at least 27% amino acid sequence identity to Csos1 (9), and all are constituents of the *S. enterica* organelles (this study) suggesting that these proteins may also be shell components of the *pdu* organelles. Likewise, the PduB, PduB′, and PduU organelle proteins are distantly related to Csos1 (9) and hence may also serve as shell components. This suggests that the shell of the *pdu* organelles may be quite complex indeed.

In addition to the putative shell proteins, four enzymes were shown to be components of the purified *pdu* organelles: Ado-B_{12}-dependent diol dehydratase (PduCDE), propionaldehyde dehydrogenase (PduP), adenosyltransferase (PduO), and a putative diol dehydratase reactivating factor (PduGH). As a group, these enzymes are sufficient to mediate the conversion of 1,2-PD to propionyl-CoA. Ado-B_{12}-dependent diol dehydratase catalyzes the conversion of 1,2-PD to propionaldehyde, which is then converted to propionyl-CoA by the CoA-dependent propionaldehyde dehydrogenase (1, 24, 37). Adenosyltransferase and the PduGH reactivating factor are needed to maintain diol dehydratase in an active form (20). Thus, the *pdu* organelles include all the enzymatic activities needed for the conversion of 1,2-PD to propionyl-CoA.

Previously, we proposed that the *pdu* organelles function to minimize aldehyde toxicity during the growth of *S. enterica* on 1,2-PD (17). Based on the findings reported here, we propose a model for how this occurs (Fig. 5) In the model, the conversion of 1,2-PD to propionyl-CoA occurs within the lumen of the organelle, but the remaining steps of 1,2-PD degradation take place in the cytoplasm of the cell. Sequestration and/or channeling assures that the majority of the propionaldehyde is converted to propionyl-CoA inside the organelle, thus protecting cytoplasmic components. This model is supported by the findings that Ado-B12-dependent diol dehydratase and propionaldehyde dehydrogenase are major organelle components, and by the fact that a putative propanol dehydrogenase (PduQ), propionate kinase (PduW), and phosphotransacylase were undetectable in the purified organelles indicating that these enzymes function in the cytoplasm of the cell (this study). In addition, since previous studies indicated that the *pdu* organelles also reduce aldehyde toxicity by regulation of diol dehydratase activity (17), it is proposed that the *pdu* organelles function via a combined mechanism of aldehyde channeling and/or sequestration augmented by control of diol dehydratase activity to fine tune aldehyde production and consumption.

The findings reported also establish the *pdu* organelles as the second example of a complex, multiprotein, polyhedral

organelle (carboxysomes being the first). This raises two interesting questions: how many different metabolic processes occur within protein-bound organelles and how widely distributed are such organelles in nature? Electron microscopy has shown that carboxysomes are produced by a number of photo- and chemoautotrophic bacteria (11, 12, 33). Polyhedral organelles have also been observed in *Salmonella*, *Klebsiella*, and *Citrobacter* during growth on 1,2-PD (9, 17, 31) (H. C. Aldrich, T. A. Bobik, D. S. Williams, and R. J. Busch, Abstr. 98th Gen. Meet. Am. Soc. Microbiol. 1998, abstr. 140J-2, 1998), and analyses of sequenced genomes (for clusters of genes related to organelle shell genes) have indicated that *pdu* organelles are also formed by *Listeria*, *Lactobacillus*, and *Clostridium*. Similar bioinformatic analyses have indicated that a polyhedral organelle is also involved in Ado-B_{12}-dependent ethanolamine utilization by *Salmonella*, *Escherichia*, *Klebsiella*, *Fusobacterium*, *Listeria*, and *Clostridium*, and electron microscopy studies have shown that *Salmonella*, *Escherichia*, and *Klebsiella* do indeed form polyhedral organelles during growth on ethanolamine (31; H. C. Aldrich et al., Abstr. 98th Gen. Meet. Am. Soc. Microbiol.). In addition, based on bioinformatic studies it appears that *Desulfitobacterium hafniense* and *Desulfovibrio desulfuricans* also have the potential to produce a polyhedral organelle. The genomes of these organisms include multiple homologues of organelle shell genes interspersed with genes of unknown function. Thus, overall, it appears that at least four different metabolic processes occur within polyhedral organelles and bioinformatic analyses indicate that 30 of 209 organisms for which partial or complete sequence data are available have the potential to express polyhedral organelles. Importantly, the possibility exists that a larger number of metabolic processes might occur within protein-bound organelles. Such organelles might have escaped prior notice because their observation would require electron microcopy of cells grown under specialized conditions as is the case for both *pdu* and *eut* organelles. Furthermore, bioinformatic analyses would fail to identify protein-bound organelles that lack homologues of known organelle proteins. Hence, protein-bound organelles may be more widespread in nature than currently thought.

ACKNOWLEDGMENTS

This work was supported by grant GM059486 from the National Institutes of Health and by the Florida Agricultural Experiment Station.

We thank Scott McClung and Charity Hartmann for performing the N-terminal sequencing and Scott McMillen and Li Zhang for conducting the MALDI-TOF analyses at the Protein Chemistry Core Facility, Biotechnology Program, University of Florida. We also thank Marjorie Chow and Alexia Lunberg for performing the 2D electrophoresis at the Molecular Biomarkers Core Facility, Biotechnology Program, University of Florida. We also acknowledge Henry C. Aldrich, Donna S. Williams, and Lorraine M. McDowell for their invaluable assistance with the electron microscopy studies and Tetsuo Toraya, Nicole A. Leal, and Celeste L. V. Johnson for providing the anti-diol dehydratase, anti-PduP, and anti-PduO antisera used in the immunoblots.

REFERENCES

1. **Abeles, R. H., and H. A. Lee.** 1961. Intramolecular oxidation-reduction requiring a cobamide coenzyme. J. Biol. Chem. **236:**2347–2350.
2. **Badger, M. R., and G. D. Price.** 2003. CO_2 concentrating mechanisms in cyanobacteria: molecular components, their diversity and evolution. J. Exp. Bot. **54:**609–622.
3. **Baker, S. H., S. C. Lorbach, M. Rodriguez-Buey, D. S. Williams, H. C. Aldrich, and J. M. Shively.** 1999. The correlation of the gene *csoS2* of the carboxysome operon with two polypeptides of the carboxysome in *Thiobacillus neapolitanus.* Arch. Microbiol. **172:**233–239.
4. **Baker, S. H., D. S. Williams, H. C. Aldrich, A. C. Gambrell, and J. M. Shively.** 2000. Identification and localization of the carboxysome peptide Csos3 and its corresponding gene in *Thiobacillus neapolitanus.* Arch. Microbiol. **173:**278–283.
5. **Banerjee, R. (ed.).** 1999. Chemistry and biochemistry of B_{12}. John Wiley and Sons, New York, N.Y.
6. **Berggren, K., E. Chernokalskaya, T. H. Steinberg, C. Kemper, M. F. Lopez, Z. Diwu, R. P. Haugland, and W. F. Patton.** 2000. Background-free, high sensitivity staining of proteins in one- and two-dimensional sodium dodecyl sulfate-polyacrylamide gels using a luminescent ruthenium complex. Electrophoresis **21:**2509–2521.
7. **Berkowitz, D., J. M. Hushon, H. J. Whitfield, Jr., J. Roth, and B. N. Ames.** 1968. Procedure for identifying nonsense mutations. J. Bacteriol. **96:**215–220.
8. **Bobik, T. A., M. Ailion, and J. R. Roth.** 1992. A single regulatory gene integrates control of vitamin B_{12} synthesis and propanediol degradation. J. Bacteriol. **174:**2253–2266.
9. **Bobik, T. A., G. D. Havemann, R. J. Busch, D. S. Williams, and H. C. Aldrich.** 1999. The propanediol utilization (*pdu*) operon of *Salmonella enterica* serovar Typhimurium LT2 includes genes necessary for formation of polyhedral organelles involved in coenzyme B_{12}-dependent 1,2-propanediol degradation. J. Bacteriol. **181:**5967–5975.
10. **Bobik, T. A., Y. Xu, R. M. Jeter, K. E. Otto, and J. R. Roth.** 1997. Propanediol utilization genes (*pdu*) of *Salmonella typhimurium*: three genes for the propanediol dehydratase. J. Bacteriol. **179:**6633–6639.
11. **Cannon, G. C., S. H. Baker, F. Soyer, D. R. Johnson, C. E. Bradburne, J. L. Mehlman, P. S. Davies, Q. L. Jiang, S. Heinhorst, and J. M. Shively.** 2003. Organization of carboxysome genes in the thiobacilli. Curr. Microbiol. **46:** 115–119.
12. **Cannon, G. C., C. E. Bradburne, H. C. Aldrich, S. H. Baker, S. Heinhorst, and J. M. Shively.** 2001. Microcompartments in prokaryotes: carboxysomes and related polyhedra. Appl. Environ. Microbiol. **67:**5351–5361.
13. **Cannon, G. C., S. Heinhorst, C. E. Bradburne, and J. M. Shively.** 2002. Carboxysome genomics: a status report. Funct. Plant Biol. **29:**175–182.
14. **Cannon, G. C., and J. M. Shively.** 1983. Characterization of a homogenous preparation of carboxysomes from *Thiobacillus neapolitanus.* Arch. Microbiol. **134:**52–59.
15. **Chen, P., M. Ailion, T. Bobik, G. Stormo, and J. Roth.** 1995. Five promoters integrate control of the *cob*/*pdu* regulon in *Salmonella typhimurium.* J. Bacteriol. **177:**5401–5410.
16. **English, R. S., S. C. Lorbach, X. Qin, and J. M. Shively.** 1994. Isolation and characterization of a carboxysome shell gene from *Thiobacillus neapolitanus.* Mol. Microbiol. **12:**647–654.
17. **Havemann, G. D., E. M. Sampson, and T. A. Bobik.** 2002. PduA is a shell protein of polyhedral organelles involved in coenzyme B_{12}-dependent degradation of 1,2-propanediol in *Salmonella enterica* serovar Typhimurium LT2. J. Bacteriol. **184:**1253–1261.
18. **Holthuijzen, Y. A., J. F. L. Vanbreemen, J. G. Kuenen, and W. N. Konings.** 1986. Protein composition of the carboxysomes of *Thiobacillus neapolitanus.* Arch. Microbiol. **144:**398–404.
19. **Jeter, R. M., and J. R. Roth.** 1987. Cobalamin (vitamin B_{12}) biosynthetic genes of *Salmonella typhimurium.* J. Bacteriol. **169:**3189–3198.
20. **Johnson, C. L., E. Pechonick, S. D. Park, G. D. Havemann, N. A. Leal, and T. A. Bobik.** 2001. Functional genomic, biochemical, and genetic characterization of the Salmonella *pduO* gene, an ATP:cob(I)alamin adenosyltransferase gene. J. Bacteriol. **183:**1577–1584.
21. **Kaplan, A., and L. Reinhold.** 1999. CO_2 concentrating mechanisms in photosynthetic microorganisms. Annu. Rev. Plant Physiol. Plant Mol. Biol. **50:** 539–550.
22. **McDowell, E. M., and B. F. Trump.** 1976. Histologic fixatives suitable for diagnostic light and electron microscopy. Arch. Pathol. Lab. Med. **100:**405–414.
23. **McGee, D. E., S. S. Carroll, M. W. Bond, and J. H. Richards.** 1982. Diol dehydratase: N-terminal amino acid sequences and subunit stoichiometry. Biochem. Biophys. Res. Commun. **108:**547–551.
24. **Obradors, N., J. Badia, L. Baldoma, and J. Aguilar.** 1988. Anaerobic metabolism of the L-rhamnose fermentation product 1,2-propanediol in *Salmonella typhimurium.* J. Bacteriol. **170:**2159–2162.
25. **Price, G. D., D. Sultemeyer, B. Klughammer, M. Ludwig, and M. R. Badger.** 1998. The functioning of the CO_2 concentrating mechanism in several cyanobacterial strains: a review of general physiological characteristics, genes, proteins, and recent advances. Can. J. Bot. **76:**973–1002.
26. **Price-Carter, M., J. Tingey, T. A. Bobik, and J. R. Roth.** 2001. The alternative electron acceptor tetrathionate supports B_{12}-dependent anaerobic growth of *Salmonella enterica* serovar typhimurium on ethanolamine or 1,2-propanediol. J. Bacteriol. **183:**2463–2475.
27. **Roth, J. R., J. G. Lawrence, and T. A. Bobik.** 1996. Cobalamin (coenzyme B_{12}): synthesis and biological significance. Annu. Rev. Microbiol. **50:**137–181.
28. **Sambrook, J., E. F. Fritsch, and T. Maniatis.** 1989. Molecular cloning: a

laboratory manual, 2nd ed. Cold Spring Harbor Laboratory, Cold Spring Harbor, N.Y.
29. **Sauvageot, N., C. Muller, A. Hartke, Y. Auffray, and J. M. Laplace.** 2002. Characterisation of the diol dehydratase *pdu* operon of *Lactobacillus collinoides.* FEMS Microbiol. Lett. **209:**69–74.
30. **Schneider, Z., and A. Stroinski.** 1987. Comprehensive B_{12}: chemistry, biochemistry, nutrition, ecology, medicine. De Gruyter, Berlin, Germany.
31. **Shively, J. M., C. E. Bradburne, H. C. Aldrich, T. A. Bobik, J. L. Mehlman, S. Jin, and S. H. Baker.** 1998. Sequence homologs of the carboxysomal polypeptide CsoS1 of the thiobacilli are present in cyanobacteria and enteric bacteria that form carboxysomes—polyhedral bodies. Can. J. Bot. **76:**906–916.
32. **Shively, J. M., and R. S. English.** 1991. The Carboxysome, a prokaryotic organelle. Can. J. Bot. **69:**957–962.
33. **Shively, J. M., G. van Keulen, and W. G. Meijer.** 1998. Something from almost nothing: carbon dioxide fixation in chemoautotrophs. Annu. Rev. Microbiol. **52:**191–230.
34. **Stojiljkovic, I., A. J. Baumler, and F. Heffron.** 1995. Ethanolamine utilization in *Salmonella typhimurium*: nucleotide sequence, protein expression, and mutational analysis of the *cchA cchB eutE eutJ eutG eutH* gene cluster. J. Bacteriol. **177:**1357–1366.
35. **Toraya, T.** 2000. Radical catalysis of B_{12} enzymes: structure, mechanism, inactivation, and reactivation of diol and glycerol dehydratases. Cell Mol. Life Sci. **57:**106–127.
36. **Toraya, T., and S. Fukui.** 1977. Immunochemical evidence for the difference between coenzyme-B_{12}-dependent diol dehydratase and glycerol dehydratase. Eur. J. Biochem. **76:**285–289.
37. **Toraya, T., S. Honda, and S. Fukui.** 1979. Fermentation of 1,2-propanediol with 1,2-ethanediol by some genera of Enterobacteriaceae, involving coenzyme B_{12}-dependent diol dehydratase. J. Bacteriol. **139:**39–47.
38. **Toraya, T., and K. Mori.** 1999. A reactivating factor for coenzyme B_{12}-dependent diol dehydratase. J. Biol. Chem. **274:**3372–3377.
39. **Toraya, T., K. Ushio, S. Fukui, and P. C. Hogenkamp.** 1977. Studies on the mechanism of the adenosylcobalamin-dependent diol dehydrase reaction by the use of analogs of the coenzyme. J. Biol. Chem. **252:**963–970.
40. **Vogel, H. J., and D. M. Bonner.** 1956. Acetylornithinase of *Escherichia coli*: partial purification and some properties. J. Biol. Chem. **218:**97–106.
41. **Zacharius, R. M., T. E. Zell, J. H. Morrison, and J. J. Woodlock.** 1969. Glycoprotein staining following electrophoresis on acrylamide gels. Anal. Biochem. **30:**148–152.
42. **Zhang, W., and B. T. Chait.** 2000. ProFound: an expert system for protein identification using mass spectrometric peptide mapping information. Anal. Chem. **72:**2482–2489.